

Kent Academic Repository

Full text document (pdf)

Citation for published version

Zhang, Quoqiang and Yan, Yong and Hu, Yonghui and Zheng, Ge (2019) On-line Size Measurement of Pneumatically Conveyed Particles Through Acoustic Emission Sensing. Powder Technology . ISSN 0032-5910. (In press)

DOI

Link to record in KAR

<https://kar.kent.ac.uk/73854/>

Document Version

Author's Accepted Manuscript

Copyright & reuse

Content in the Kent Academic Repository is made available for research purposes. Unless otherwise stated all content is protected by copyright and in the absence of an open licence (eg Creative Commons), permissions for further reuse of content should be sought from the publisher, author or other copyright holder.

Versions of research

The version in the Kent Academic Repository may differ from the final published version.

Users are advised to check <http://kar.kent.ac.uk> for the status of the paper. **Users should always cite the published version of record.**

Enquiries

For any further enquiries regarding the licence status of this document, please contact:

researchsupport@kent.ac.uk

If you believe this document infringes copyright then please contact the KAR admin team with the take-down information provided at <http://kar.kent.ac.uk/contact.html>

On-line Size Measurement of Pneumatically Conveyed Particles Through Acoustic Emission Sensing

Authors: Guoqiang Zhang ^a
Yong Yan ^b (Corresponding author)
Yonghui Hu ^a
Ge Zheng ^a

Addresses: ^a School of Control and Computer Engineering
North China Electric Power University
Beijing 102206
P. R. China

^b School of Engineering and Digital Arts
University of Kent
Canterbury
Kent CT2 7NT
UK
Tel: 00441227823015
Fax: 00441227456084
Email: y.yan@kent.ac.uk

ABSTRACT

Acoustic emission (AE) methods have been proposed for on-line size measurement of pneumatically conveyed particles in recent years. However, there is limited research on the fundamental mechanism of the AE-based particle sizing technique. In order to achieve more accurate measurement of particle size, the impact between particles and a waveguide should be described in a more realistic way. In this paper, an improved model based on the Stronge impact theory is presented to establish the relationship between the resulting AE signal and the particle size being measured. The improved model is validated with experiments on a single-particle test rig. A total five sets of glass beads with a mean diameter of 0.4, 0.6, 0.8, 1.0 and 1.2 mm, respectively, are used as the test particles with an impact velocity ranging from 22 m/s to 37 m/s. It is proven that the Stronge impact theory is more accurate to describe the collision process than the Hertzian impact theory and is thus more suitable for the particle size inversion, which is validated by comparing the inversion results using these two impact theories. Meanwhile, a good agreement is observed between the measured and reference particle sizes under different experimental conditions. The mean relative error between the measured and reference diameters is mostly within 12%.

Keywords – particle size, acoustic emission, single particle, Stronge impact theory, plastic deformation.

I. INTRODUCTION

The measurement of particle size is required in many industrial processes. For example, it is important to monitor the size distribution of pulverized fuel (coal and biomass) in the power generation industry, as it relates to combustion stability, pollutant emissions and process efficiency of a utility boiler [1, 2]. A variety of techniques have been developed for the

measurement of particle size, such as laser diffraction [3], ultrasound [4], digital imaging [5] and acoustic emission (AE) detection [6]. Among these techniques, the AE method is considered as a promising approach to on-line sizing of pneumatically conveyed particles. The advantages of the AE method include high sensitivity, on-line measurement, easy installation and low maintenance.

Some preliminary research on the AE method has been performed and the validity of this approach has been demonstrated by experimental results [7-11]. Leach and Rubin [7] used AE signals for particle sizing by analysing the acoustic frequencies of the impact among particles. However, this method is only appropriate for spherical particles. Buttle *et al.* [8] developed two methods for particle size measurement by quantitative acoustic emission. The first one incorporates the peak amplitude of the AE signal and other collision information such as impact velocity, incident angle and coefficient of restitution. The second one mainly relies on the rise time of the AE signal without using any information of the particle dynamics. Although satisfactory results were obtained, the sophisticated measuring system and tedious calibration process restrict its industrial applications. Bastari *et al.* [9] collected the AE signals due to the impacts of coal powder with an intrusive probe and introduced a system identification technique to achieve particle size distribution measurement on a power station. Uher *et al.* [10] and Gao *et al.* [11] modelled and validated the relationship between the resulting AE signal and the particle size using the Hertzian impact theory. The results obtained under different experimental conditions have shown the feasibility of the AE method for measurement of particle size distribution.

However, there are still some unsolved challenges related to the measurement accuracy of the AE method. Firstly, in current studies the Hertzian impact theory is usually used to describe the collision of solid bodies, which assumes that the contact is perfectly elastic during the impact. But

in fact, plastic deformation and energy loss always occur. Especially when the impact velocity is high, the Hertzian impact theory is no longer suitable for describing the collision process [12]. The plasticity directly influences the estimation of contact force during the impact, leading to measurement errors of the particle size. Secondly, as the experiments were usually carried out with particles in pneumatic conveying pipelines [13], the inevitable overlap of collisions makes it difficult to separate the individual impact events for particle sizing, which leads to increased measurement errors. In addition, the detected AE signal is also influenced by the environmental noise and the vibration of the pneumatic conveying pipe, which cause difficulties for signal analysis and particle size inversion. Although it is very hard to eliminate these factors in practical situations, their effects on the measured AE signal should be taken into account for a better understanding of the measurement mechanism.

In order to establish the relationship between the features of the AE signal and the characteristics of the particle such as particle size and impact velocity, the AE signal from a single impact event is collected under well-controlled conditions. McLaskey and Glaser [14] studied the impact problem that a ball impacts on a massive plate using an array of high-fidelity piezoelectric sensors and the collected AE signals were compared with the theoretical signals from the Hertzian impact theory. The plastic deformation during the collision was also qualitatively discussed. He *et al.* [15] found that the AE signal produced from a particle impacting on a plate contains the information on both particle-wall collision and particle-wall friction as the impact is not perfectly perpendicular to the plate. Požar *et al.* [16] measured accurately the contact time of a normal-incidence sphere with a transparent glass block and validated the linear relationship between the contact time and the particle size. Coombes and Yan [17] carried out a single-particle-impact experiment using free-fall particles colliding onto a waveguide with a very small impact area and

investigated the collected AE signal through power spectral analysis. In a similar way, Hayashi *et al.* [18] found that the AE signal from collision of a single impact contains two main frequency peaks, the amplitude ratio of which depends on the particle size. As the impact of a single particle can be used to obtain the full waveform of the AE event, it is therefore possible to gain a better understanding of the AE process and hence improved measurement accuracy.

In this study, the Stronge impact theory is utilized to model the impact of a particle onto a waveguide, which takes plastic deformation into account and is more accordant with the practical situation. After that, a comprehensive approach based on the Stronge impact theory is presented to establish the relationship between the particle size and the peak AE amplitude, which is proven to be effective by single-particle-impact experiments. The experiments were carried out on an AE particle sizing rig designed for impact of single spherical particle on a waveguide. Using the test rig, it is guaranteed that there is only one particle collision occurring and the variables (i.e. particle size, impact velocity and impact location) affecting the AE signals are more controllable. Glass beads with different mean diameters were used as ideal particles. More accurate results of particle size inversion are observed based on the new theory compared with those using the Hertzian impact theory. The influence of particle size and impact velocity on the AE signal is also investigated.

II. METHODOLOGY

A. General Principle

In an AE-based particle sizing system, a metallic waveguide is introduced into the particle flow, as illustrated in Fig. 1. When the particles collide with the waveguide, transient elastic stress waves are generated at the collision point. As the waves propagate along the waveguide,

mechanical disturbance is generated on the surface, which is transformed into an electric signal by the AE sensor attached to the waveguide but located some distance away from the impact point [19]. The features of the AE signal are closely related to the impulsive force that the particle imposes on the waveguide. One of the main factors affecting the impact force is the particle size, thus offering the possibility of deriving particle size information through analysis of the AE signal.

In fact, the AE signals collected are shaped by a chain of different effects, including the source effects, wave propagation effects and instrumentation effects, as illustrated schematically in Fig. 2. Therefore, the measured AE signal is no longer the original AE source signal.

Assuming that the wave propagation medium and the instrument are linear, time-invariant systems, the measured AE signal can be expressed in time domain as [20]

$$V(t) = S(t) * G(t) * R(t) \quad (1)$$

Where $V(t)$ is the measured AE signal and $S(t)$, $G(t)$ and $R(t)$ are the functions of source effects, wave propagation effects and instrument response effects, respectively. The symbol $*$ represents convolution.

The wave propagation effects $G(t)$ describe the dynamic displacement temporally and spatially, resulting from a unit impulsive force acting on the surface of a material. The propagation of elastic waves in homogeneous materials is usually modeled by the elastodynamic equations, the solutions to which are called the Green's function [21, 22]. The instrument response effects $R(t)$ represent the response of the recording system, including the AE sensor, the cables and the signal acquisition device. If the wave propagation effects $G(t)$ and the instrument response effects $R(t)$ are known, the source effects $S(t)$ can be determined by removing the wave propagation and instrument response effects from the measured AE signal through deconvolution. The particle size information is then extracted from the derived source effects. However, the determination of

quantitative wave propagation and instrument response effects are both very challenging as they require precise modeling of the physical process and accurate calibration of the recording system. As a result, a particle sizing approach based on the peak amplitude of individual AE signal is utilized for particle size inversion in the paper.

B. Impact Modelling

As the AE source in this study is the impact between a particle and the plane of the waveguide, the source effects $S(t)$ can be described by impact theories. In existing research, the Hertzian impact theory is commonly used to describe the collision process, which assumes that the contact is both ideally normal and elastic. According to the Hertzian impact theory, the contact force during the impact of a sphere with a plane surface can be expressed as [23]

$$S(t) = \frac{4}{3} KR^{\frac{1}{2}} \alpha(t)^{\frac{3}{2}} \quad (2)$$

where R is the radius of the impacting particle and α is the deformation displacement as a function of time t . K is a constant expressed as

$$K = \left(\frac{1 - \mu_1^2}{E_1} + \frac{1 - \mu_2^2}{E_2} \right)^{-1} \quad (3)$$

where E_i is Young's modulus, μ_i is Poisson's ratio, and subscripts 1 and 2 refer to the impacting particle and plane surface, respectively.

However, plastic deformation always occurs in practical impact events, even at very low velocities [24]. In general, a higher velocity leads to more severe plastic deformation. In the current research, the velocity of particles is more than 20 m/s, which results in non-negligible plastic deformation and thus an impact theory that takes into account the plasticity should be adopted.

The Stronge impact theory divides the compression process into three distinct stages, namely

the full-elastic stage, the elastic-plastic stage and the full-plastic stage, while the recovery process is still fully elastic [25]. According to this theory, the contact force during the compression can be expressed as

$$S(t) = \begin{cases} \frac{4}{3} KR^{\frac{1}{2}} \alpha(t)^{\frac{3}{2}} & 0 \leq \alpha(t) < \alpha_{ep} \\ S_{ep} \left[\frac{2\alpha(t)}{\alpha_{ep}} - 1 \right] \left[1 + \frac{1}{3.3} \ln \frac{2\alpha(t) - \alpha_{ep}}{\alpha_{ep}} \right] & \alpha_{ep} \leq \alpha(t) < \alpha_p \\ S_{ep} \frac{b_2}{b_1} \left[\frac{2\alpha(t)}{\alpha_{ep}} - 1 \right] & \alpha(t) \geq \alpha_p \end{cases} \quad (4)$$

where S_{ep} and α_{ep} are the critical contact force and the critical deformation displacement, respectively, between the elastic and elastic-plastic regimes. α_p is the critical deformation displacement between the elastic-plastic and full-plastic regimes. The values of b_1 and b_2 are usually 1.1 and 2.7-3.0, respectively. α_{ep} and α_p can be calculated from

$$\begin{cases} \alpha_{ep} = \left(\frac{3\pi b_1 \sigma_Y}{4K} \right)^2 R \\ \alpha_p = 0.5\alpha_{ep} \left[e^{2.25(b_2 - b_1)^2} + 1 \right] \end{cases} \quad (5)$$

where σ_Y is the yield stress of the particle, which follows the relationship $\sigma_Y \propto R^{-\frac{1}{2}}$ [26].

Assuming that the collision only happens in the normal direction of the plane surface and the particle is spherical, the motion of the particle can be described by Newton's second law

$$S(t) = -m \frac{d^2 \alpha(t)}{dt^2} \quad (6)$$

where m is the mass of the particle.

By inserting the contact force based on Hertzian impact theory or Stronge impact theory into equation (6), the force-time relationship of the impact process can be derived numerically. Fig. 3

shows the force pulses for a glass bead (the diameter D is 1.0 mm and the impact velocity v is 22 m/s) acting on a stainless steel plate based on the two impact theories, respectively. The maximum contact force with Stronge impact theory is significantly lower than that derived from Hertzian impact theory, which is caused by the energy loss during the collision process. The plastic impact stage also extends the impact duration, leading to lower frequency of the AE signal.

C. Particle Size Inversion

When a particle impacts onto a waveguide, an impulsive force is produced due to the contact between the particle and the surface of the waveguide, which is closely related to the particle size. The transient elastic stress waves generated during the collision propagate along the waveguide and are eventually converted into an electric signal via the AE sensor. As a result, the amplitude of the measured AE signal is greatly affected by the impact force, which contains the particle size information. With the assumption that both the wave propagation and instrument effects can be regarded as linear, time-invariant systems, the peak amplitude of the AE signal V_{max} depends on the maximum deformation α_{max} and is proportional to the maximum contact force S_{max} during the impact process, i.e.,

$$V_{max} = A_{sys} S_{max} \quad (7)$$

where A_{sys} is a proportionality parameter of the measurement system, which is determined through static calibration. Knowing A_{sys} , the particle size can be derived from V_{max} using equations (4)-(7).

III. EXPERIMENTAL RESULTS AND DISCUSSION

A. *Experimental Setup*

A test rig that allows the impact of a single particle on the waveguide was designed and built. The schematic of the single-particle test rig is illustrated in Fig. 4. Particles are introduced individually into the open breech and then accelerated along a 110-mm-long tube with an adjustable driving pressure from the air compressor. The diameter of the open breech is 1.5 mm and the launching tube has an inner diameter of 2 mm. The signal from the AE sensor is amplified via a pre-amplifier with a bandwidth of 10 kHz-1 MHz and a gain of 20 dB to reduce the effects of noise and interference. A holographic acoustic emission signal analyser (DS-4A, Softland) is used to acquire the waveforms at a sampling frequency of 3 MHz. Meanwhile, two ring-shaped electrostatic electrodes in the upstream of the waveguide are used to determine the particle velocity through cross correlation signal processing [27]. The electrodes have a width of 3 mm, an inner diameter of 38 mm and a spacing of 40 mm between them. Fig. 5 shows the details of the experimental setup.

The waveguide is a rod made of stainless steel with a total length of 187 mm. It is semi-cylindrical with a flat surface of 50 mm in length and 10 mm in width facing the flow in the front section, which enables normal particle impact. The middle section is cylindrical, sealed with rubber bushings for isolation of the structural vibration. In the end section, the waveguide is also semi-cylindrical (25 mm long and 20 mm wide) but with opposite direction of the flat surface, to which the AE sensor is attached. The AE sensor (Nano30, PAC) is a miniature sensor, with a normal operating frequency of 125-750 kHz and resonance frequency of 300 kHz. As the AE sensor used only has a diameter of 5.5 mm, the aperture effect can be negligible. The waveguide and AE sensor are shown in Fig. 6.

B. Experimental Conditions and System Calibration

A total five sets of glass beads with a mean diameter of 0.4 mm, 0.6 mm, 0.8 mm, 1.0 mm and 1.2 mm, respectively, were used in the experiments. The experimental conditions are listed in Table I. The diameter of each particle tested was measured by a micrometer (the resolution is 0.001 mm) before launching for reference, and tests were repeated 10 times under each experimental condition. Different particle velocities were obtained by adjusting the output pressure of the air compressor. Each set of glass beads was tested under three average velocities at 22 m/s, 32 m/s and 37 m/s.

The single-particle test system was calibrated to determine A_{sys} for particle size inversion. Another five sets of glass beads with a velocity of 22 m/s were tested for calibration (ten particles for each set with a mean diameter of 0.4, 0.6, 0.8, 1.0 and 1.2 mm, respectively). According to the measurement principle, different values of A_{sys} were obtained and eventually the mean value of A_{sys} is regarded as the proportionality parameter of the system. The calculated values of A_{sys} are shown in Fig. 7. As can be seen, the calculated values of A_{sys} are generally around the mean value, which indicates that this mean value can be used as the proportionality parameter of the measurement system for particle size inversion.

C. Results and Discussion

The AE signal obtained from a single impact event is shown in Fig. 8. The diameter of the glass bead is 0.6 mm and the impact velocity is 32 m/s. It is evident that the AE signal is of impulsive nature. The background noise is also shown in Fig. 8 (a). The amplitude of the noise is very low in comparison with the AE signal. In fact, the amplitude of the noise observed is no greater than 6 mV during the experimental process whilst the AE signal has a peak amplitude of 5.7 V. Besides, no obvious noise is observed when just blowing the air flow onto the waveguide.

Therefore, the influence of environment noise and air flow is negligible in this study. Fig. 8 (b) shows a close-up view of the impact signal. The AE signal reaches the peak voltage quickly and then gradually decays with the time. By means of single particle impact, multi-particle collision is avoided and the full AE signal of particle impact can be acquired for further analysis.

Fig. 9 depicts the mean peak amplitude of the AE signals generated by different sets of particles at different velocities. It can be clearly seen that the mean peak amplitude increases with both the particle size and the impact velocity. According to the measurement principle, a greater contact force is produced when the impinging particle has a larger size or a higher velocity, thus leading to a higher peak amplitude. As the impact velocity is known, the particle size can be determined from the peak amplitude of the measured AE signal.

In order to compare the Hertzian and the Stronge impact models, the peak amplitude data at 32 m/s for five different sizes of particles are processed for particle size inversion. Fig. 10 shows the comparison between the results of particle size inversion using the two models. It is evident that the measured particle size based on the Hertzian impact theory generally yields a more significant deviation from the reference, except the 0.6 mm particles. The main reason for this is that the high impact velocity (>20 m/s) causes irreversible deformation and energy loss during the collision, when the Hertzian impact theory is no longer suitable. By contrast, the results using the Stronge impact theory agree well with the reference particle size. The average relative error of the inversion results is illustrated in Fig. 11. The relative error of the results based on the Stronge theory is much lower than those based on the Hertzian theory for most particles. Therefore, the Strong impact theory is more suitable for the particle size inversion.

Fig. 12 shows particle size inversion results for different sized particles at different velocities. As can be seen, the measured particle size shows good agreement for all particles at different

velocities. The measured particle size for 0.4 mm and 0.6 mm glass beads at a velocity of 22 m/s is smaller than the reference, which is caused by the fact that the experimental conditions are less controllable for small particles with low velocities, resulting in larger relative errors. In addition, the measurement of particle size using the micrometer by hand also tends to yield larger relative error for small particles. It is noticeable that the particle size inversion results for 1.2 mm glass beads also deviate from the reference particle size at the velocity of 32 m/s and 37 m/s. This can be explained that some slight breakage may happen in the surface of particles during the collision at high velocities as bigger glass beads tend to be broken easily. If the breakage occurs, the amplitude of the AE signal will be smaller than expected, leading to smaller measured particle size. It should be emphasized that particle fragmentation is unavoidable during the impact of particulate material with the waveguide in the pneumatic conveying pipeline, which affects the measurement accuracy for particle sizing. The effect of particle breakage on the measurement of particle size need to be studied in detail, which is beyond the scope of this paper.

Fig. 13 illustrates the mean relative error and standard deviation of the experiment results. For all the tested particles at different velocities, the mean relative error between the measured and reference particle sizes is mostly within 12% whilst the standard deviation is within 4%. The results obtained demonstrate that the Stronge impact theory can well be applied to the on-line measurement of particle size through the AE method with a reasonably good accuracy and a good repeatability.

It should be pointed out that the results in this paper are obtained under well controlled laboratory conditions in order to assess and quantify the performance and efficacy of the proposed on-line particle sizing methodology against reliable references. However, for practical industrial applications of the proposed methodology, several issues have to be considered in the

design and implementation of the AE based particle sizing system. Firstly, simultaneous multi-particle collisions with the waveguide can occur, making it difficult to separate individual impact events for particle size inversion. For this reason, the proposed method is applicable to on-line sizing of particles in dilute-phase pneumatic conveying pipelines. For instance, the particle concentration of pulverized coal in a typical power station pipeline is less than 0.1% by volume [28], which means the chance of simultaneous multi-particle collisions with the waveguide is low, particularly for larger particles. Secondly, as pulverized coal is usually in the form of spherical type [29], it is reasonable to assume spherical particles for the purpose of particle size inversion. In cases where the particles are irregular in shape, a threshold-based signal processing approach [30] may be applied to deal with this particulate problem. Meanwhile, an appropriate denoising method has to be employed in order to extract useful information for on-line particle sizing from the AE signals which may be contaminated by strong background noise. These aspects of practical applications of the developed methodology will be addressed in the near future.

IV. CONCLUSION

In this paper, an improved approach based on the Stronge impact theory has been presented to realize particle size measurement through AE sensing and its validity verified on a single-particle test rig. The Stronge impact theory is used to describe the collision of a spherical particle onto a plane surface, as the plasticity has a significant effect on the contact force and impact duration. It is proven that, in comparison with the Herzian impact theory, the Stronge impact theory is advantageous on the particle size inversion in terms of measurement accuracy. For all the five sets of tested particles, the measured particle size is in a good agreement with the reference over the

velocity range of 22-37 m/s. The mean relative error between the measured and reference particle size is mostly within 12% with a normalized standard deviation within 4%. The results obtained have indicated that the approach has the potential to be applied for on-line size measurement of particles in dilute pneumatic conveying pipelines. An industrial prototype for on-line particle sizing based on the proposed methodology will be constructed and evaluated on a full-scale coal fired power station in the near future.

ACKNOWLEDGMENT

The authors wish to acknowledge the National Natural Science Foundation of China (Nos. 61573140 and 61673170) for providing financial support. Guoqiang Zhang also would like to thank the China Scholarship Council for providing a fellowship to visit the University of Kent.

REFERENCES

- [1] Y. Ninomiya, L. Zhang, A. Sato, Z. Dong, Influence of coal particle size on particulate matter emission and its chemical species produced during coal combustion, *Fuel Process. Technol.* 85 (2004) 1065-1088.
- [2] H. Lu, E. Ip, J. Scott, P. Foster, M. Vickers, L. Baxter, Effects of particle shape and size on devolatilization of biomass particle, *Fuel* 89 (2010) 1156-1168.
- [3] D. L. Black, Q. M. Mardson, M. P. Bonin, Laser-based technique for particle-size measurement: A review of sizing methods and their industrial application, *Prog. Energy Combust. Sci.* 22 (1996) 267-306.
- [4] M. Su, M. Xue, X. Cai, Z. Shang, F. Xu, Particle size characterization by ultrasonic attenuation spectra, *Particuology* 6 (2008) 276-281.

- [5] R. M. Carter, Y. Yan, P. Lee, On-line nonintrusive measurement of particle size distribution through digital imaging, *IEEE Trans. Instrum. Meas.* 55 (2006) 2034-2038.
- [6] J. W. R. Boyd, J. Varley, The uses of passive measurement of acoustic emissions from chemical engineering processes, *Chem. Eng. Sci.* 56 (2001) 1749-1767.
- [7] M. F. Leach, G. A. Rubin, Particle size determination from acoustic emissions, *Powder Technol.* 16 (1977) 153-158.
- [8] D. J. Buttle, S. R. Martin, C. B. Scruby, Particle sizing by quantitative acoustic emission, *Res. Nondestr. Eval.* 3 (1991) 1-26.
- [9] A. Bastari, C. Cristalli, R. Morlacchi, E. Pomponi, Acoustic emissions for particle sizing of powders through signal processing techniques, *Mech. Syst. Signal Process* 25 (2011) 901-916.
- [10] M. Uher, P. Beneš, Measurement of particle size distribution by the use of acoustic emission method, *Proc. IEEE Int. Instrum. Meas. Technol. Conf.* (2012) 1194-1198, Graz, Austria.
- [11] L. Gao, Y. Yan, R. M. Carter, D. Sun, P. Lee, C. Xu, On-line particle sizing of pneumatically conveyed biomass particles using piezoelectric sensors, *Fuel* 113 (2013) 810-816.
- [12] P. Müller, M. Trüe, B. Böttcher, J. Tomas, Acoustic evaluation of the impact of moist spherical granules and glass beads, *Powder Technol.* 278 (2015) 138-149.
- [13] Y. Hu, X. Qian, X. Huang, L. Gao, Y. Yan, Online continuous measurement of the size distribution of pneumatically conveyed particles by acoustic emission methods, *Flow Meas. Instrum.* 40 (2014) 163-168.

- [14] G. C. McLaskey, S. D. Glaser, Hertzian impact: Experimental study of the force pulse and resulting stress waves, *J. Acoust. Soc. Am.* 128 (2010) 1087-1096.
- [15] L. He, Y. Zhou, Z. Huang, J. Wang, M. Lungu, Y. Yang, Acoustic analysis of particle-wall interaction and detection of particle mass flow rate in vertical pneumatic conveying, *Ind. Eng. Chem. Res.* 53 (2014) 9938-9948.
- [16] T. Požar, J. Rus, R. Petkovšek, Optical detection of impact contact times with a beam deflection probe, *Exp. Mech.* 57 (2017) 1225-1238.
- [17] J. R. Coombes, Y. Yan, Experimental investigations into the use of piezoelectric film transducers to determine particle size through impact analysis, *Proc. IEEE Int. Instrum. Meas. Technol. Conf.* (2016) 1-6, Taipei.
- [18] M. Hayashi, T. Kikkawa, D. Koyama, M. Matsukawa, Piezoelectric particle sizer for measuring bed load using a combination of resonance vibration modes, *Sens. Actuators, A* 267 (2017) 150-155.
- [19] C. B. Scruby, An introduction to acoustic emission, *J. Phys. E: Sci. Instrum.* 20 (1987) 946-953.
- [20] G. C. McLaskey, S. D. Glaser, Acoustic emission sensor calibration for absolute source measurements, *J. Nondestr. Eval.* 31 (2012) 157-168.
- [21] W. Pardee, Acoustic emission and the plate Green's function, *J. Math. Phys.* 18 (1977) 676-686.
- [22] A. N. Ceranoglu, Y. Pao, Propagation of elastic pulses and acoustic emission in a plate-part 1: theory, *J. Appl. Mech.* 48 (1981) 125-132.
- [23] J. Reed, Energy losses due to elastic wave propagation during an elastic impact, *J. Phys. D: Appl. Phys.* 18 (1985) 2329-2337.

- [24] K. L. Johnson, *Contact Mechanics*, 1st edition. Cambridge, UK: Cambridge University Press, 1987.
- [25] W. J. Stronge, *Impact Mechanics*, 1st edition. Cambridge, UK: Cambridge University Press, 2004.
- [26] J. Litster, *Design and Processing of Particulate Products*, 1st edition. Cambridge, UK: Cambridge University Press, 2016.
- [27] X. Qian, Y. Yan, J. Shao, L. Wang, H. Zhou, C. Wang, Quantitative characterization of pulverized coal and biomass–coal blends in pneumatic conveying pipelines using electrostatic sensor arrays and data fusion techniques, *Meas. Sci. Technol.* 23 (2012) 085307-1-085307-13.
- [28] Y. Yan, Guide to the flow measurement of particulate solid in pipelines, part 1: fundamentals and principles, *Powder Handling Process.* 13 (2001) 343-352.
- [29] J. P. Mathews, S. Eser, P. G. Hatcher, A. W. Scaroni, The shape of pulverized bituminous vitrinite coal particles, *KONA Powder Part. J.* 25 (2007) 145-152.
- [30] E. Nsugbe, A. Starr, I. Jennions, C. R. Carcel, Particle size distribution estimation of a mixture of regular and irregular sized particles using acoustic emissions, *Procedia Manuf.* 11 (2017) 2252-2259.

List of Figures:

Fig. 1. Schematic illustration of particle sizing by the AE method.

Fig. 2. Block diagram of the signal.

Fig. 3. Force-time curves based on Hertzian impact theory and Stronge impact theory (glass bead, $D=1.0$ mm, $v=22$ m/s).

Fig. 4. Schematic of the single particle impact system.

Fig. 5. Experimental setup.

Fig. 6. The waveguide and AE sensor.

Fig. 7. A_{sys} for different particle sizes (glass bead, $v=22$ m/s).

Fig. 8. AE signal generated in a single impact event (glass bead, $D=0.6$ mm, $v=32$ m/s).

Fig. 9. Mean peak amplitudes of the AE signals for different velocities.

Fig. 10. Particle size inversion results using the two impact models (glass bead, $v=32$ m/s).

Fig. 11. Mean relative error of particle size inversion results.

Fig. 12. Particle size inversion results.

Fig. 13. Mean relative error with standard deviation for different particle sizes.

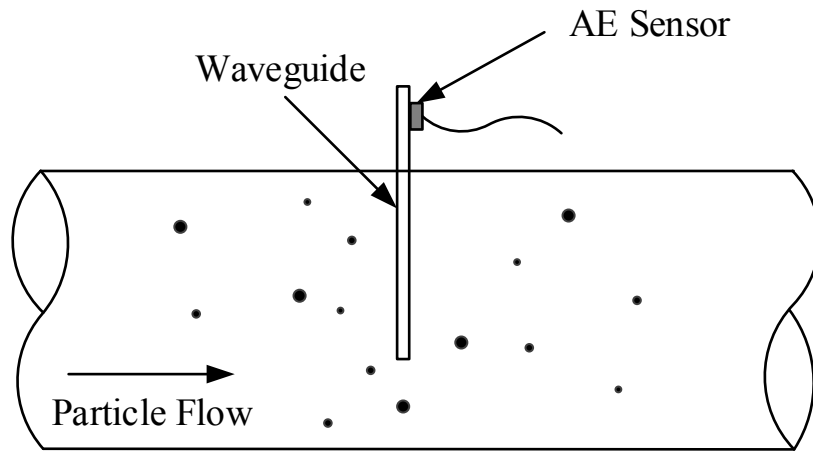


Fig. 1. Schematic illustration of particle sizing by the AE method.

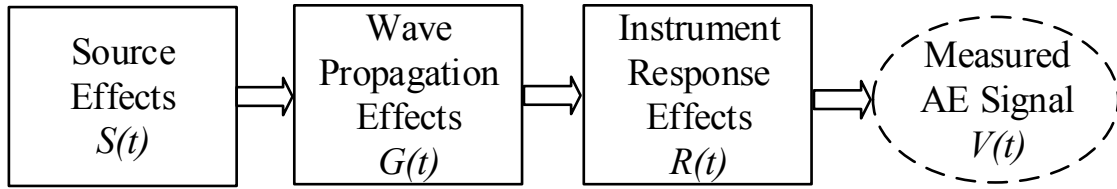


Fig. 2. Block diagram of the signal.

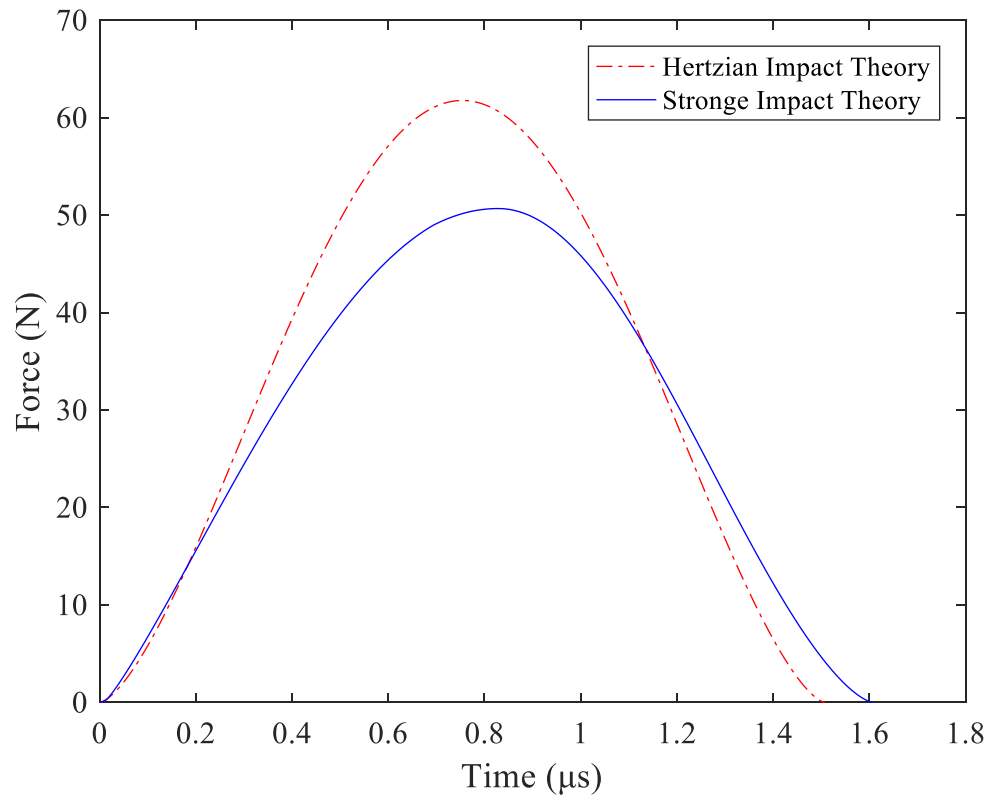


Fig. 3. Force-time curves based on Hertzian impact theory and Stronge impact theory (glass bead, $D=1.0$ mm, $v=22$ m/s).

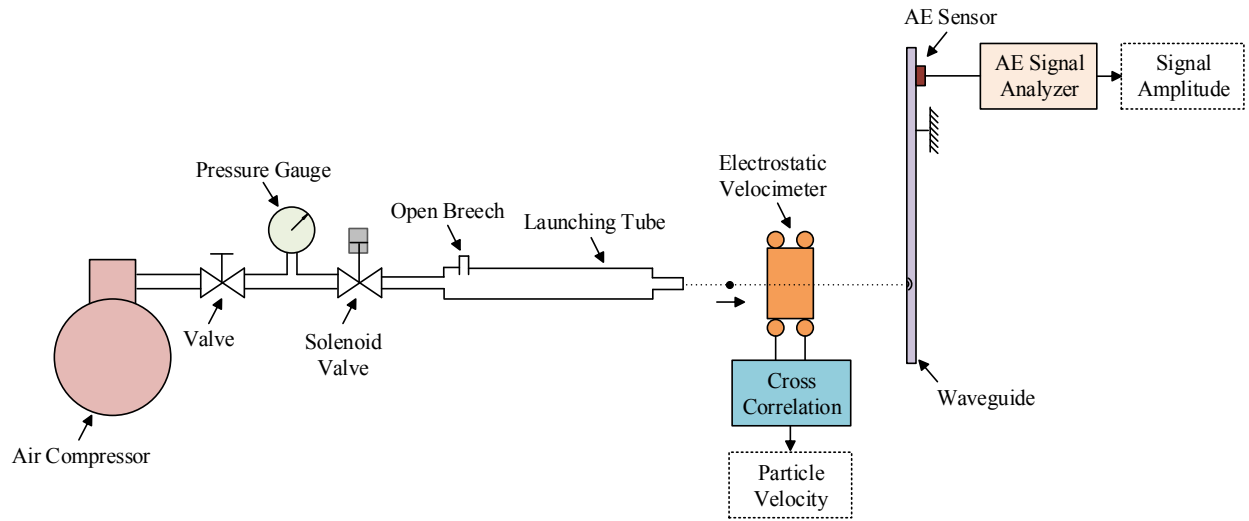


Fig. 4. Schematic of the single particle impact system.

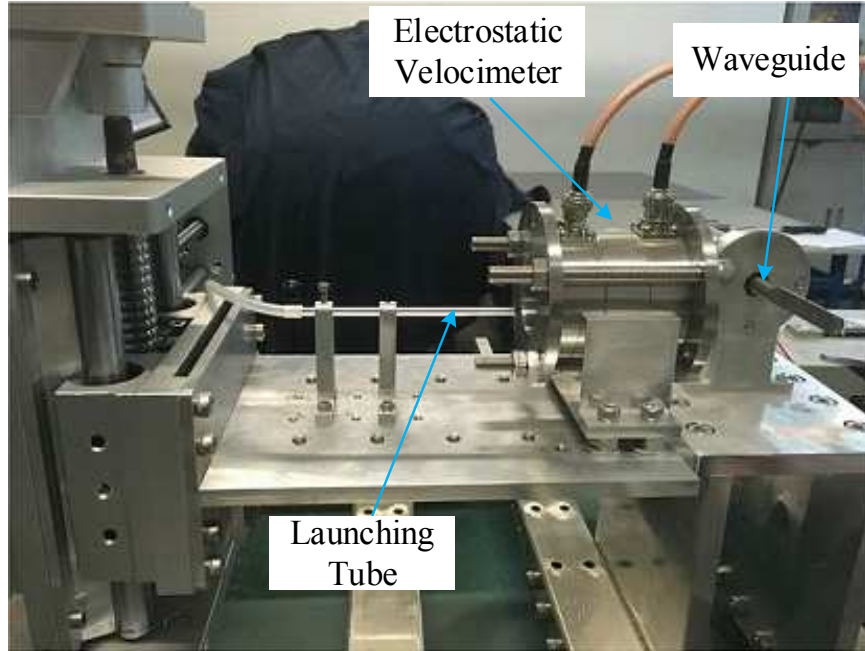


Fig. 5. Experimental setup.

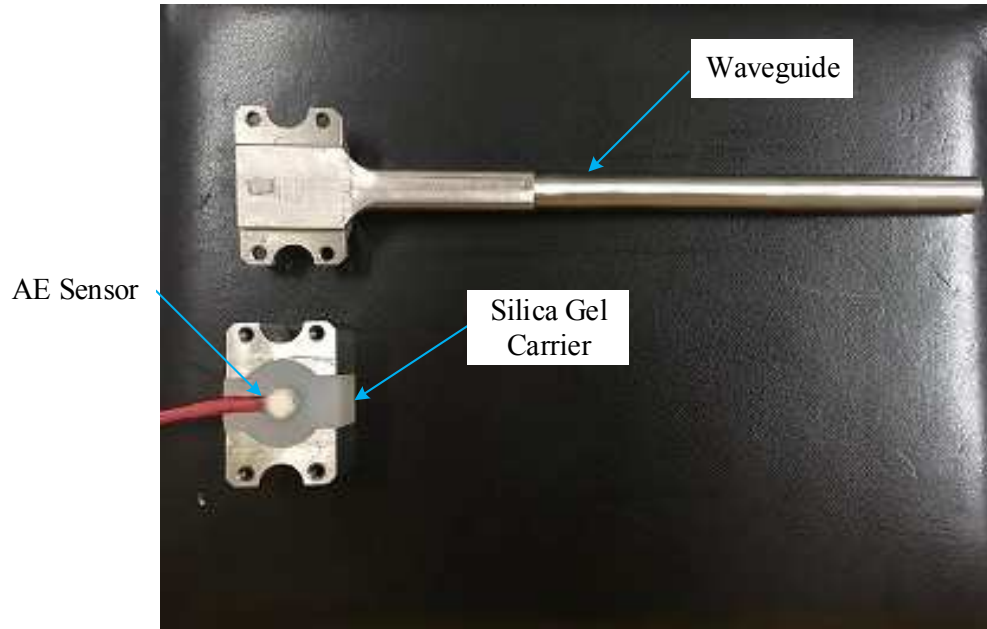


Fig. 6. The waveguide and AE sensor.

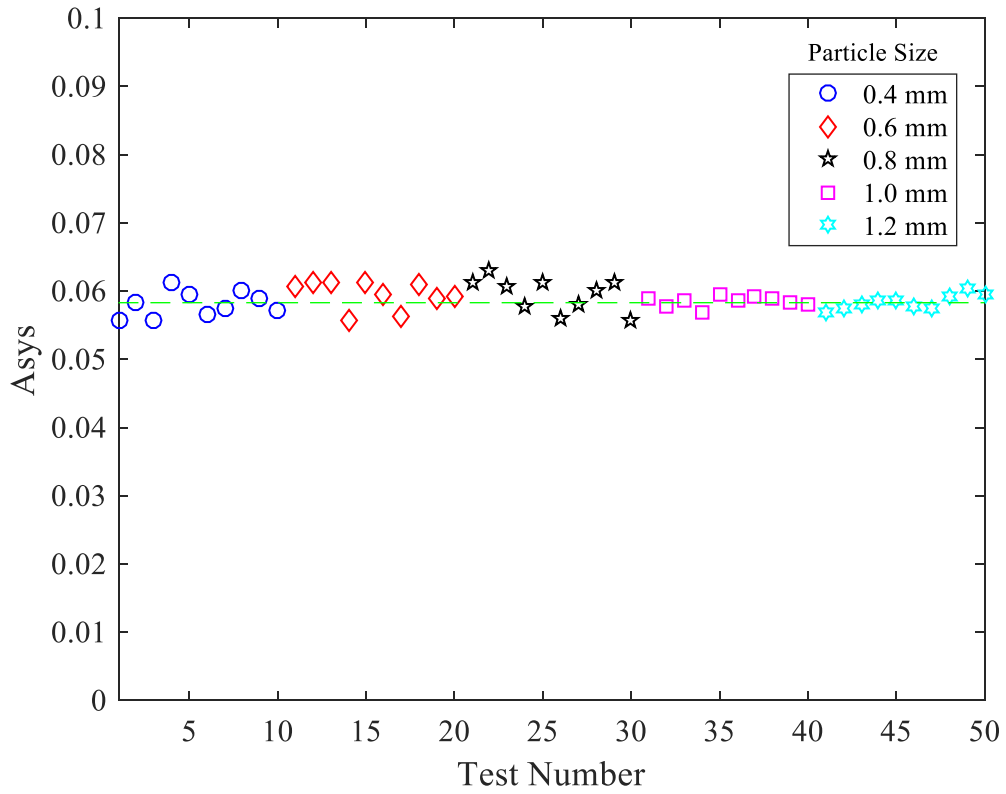
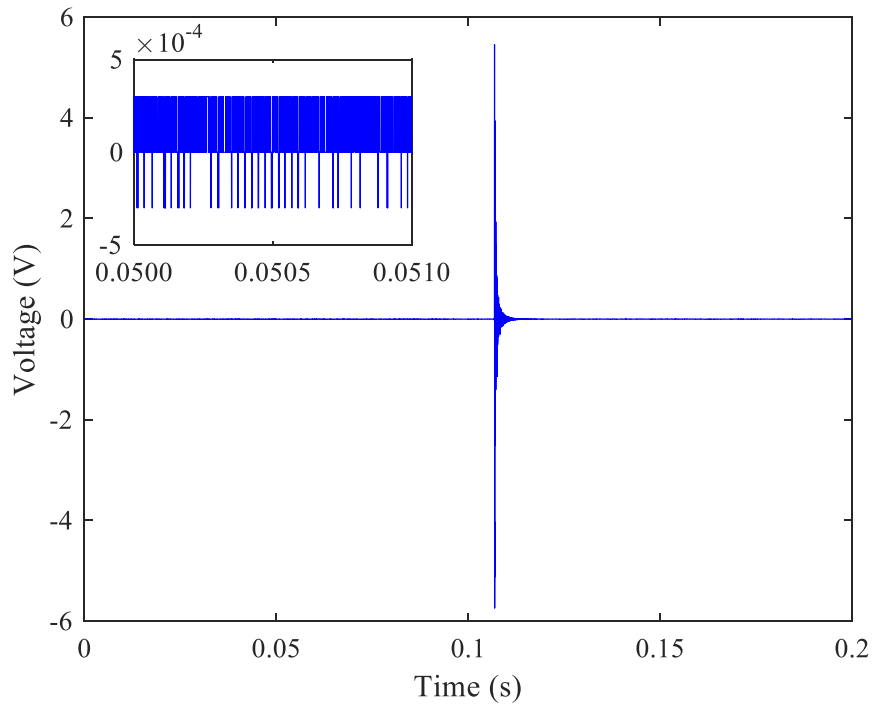
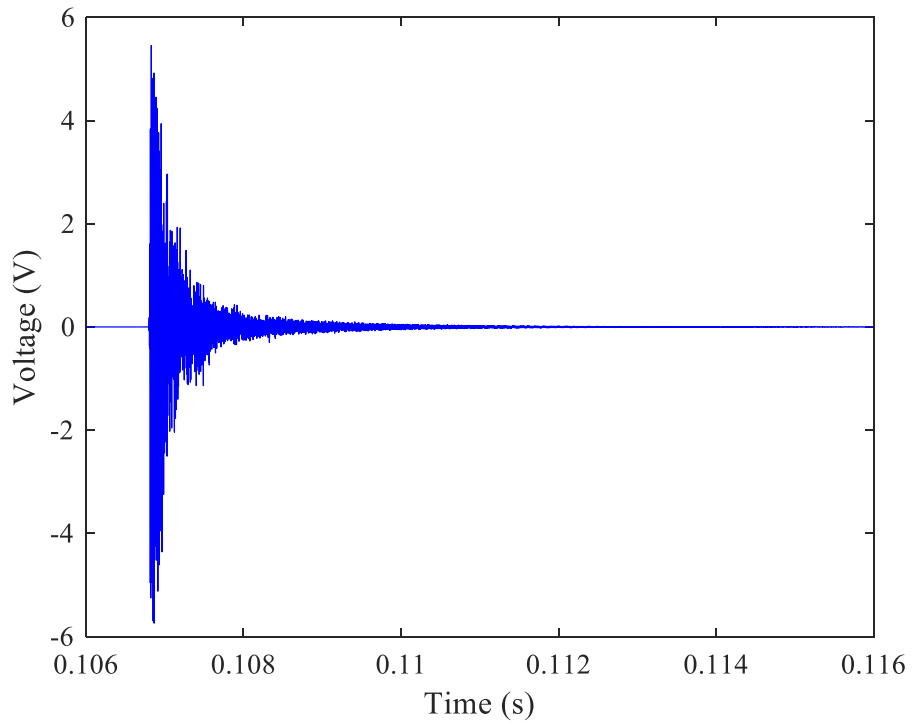


Fig. 7. A_{sys} for different particle sizes (glass bead, $v=22$ m/s).



(a) AE signal over 0.2 s



(b) A close-up view of the impact event

Fig. 8. AE signal generated in a single impact event (glass bead, $D=0.6$ mm, $v=32$ m/s).

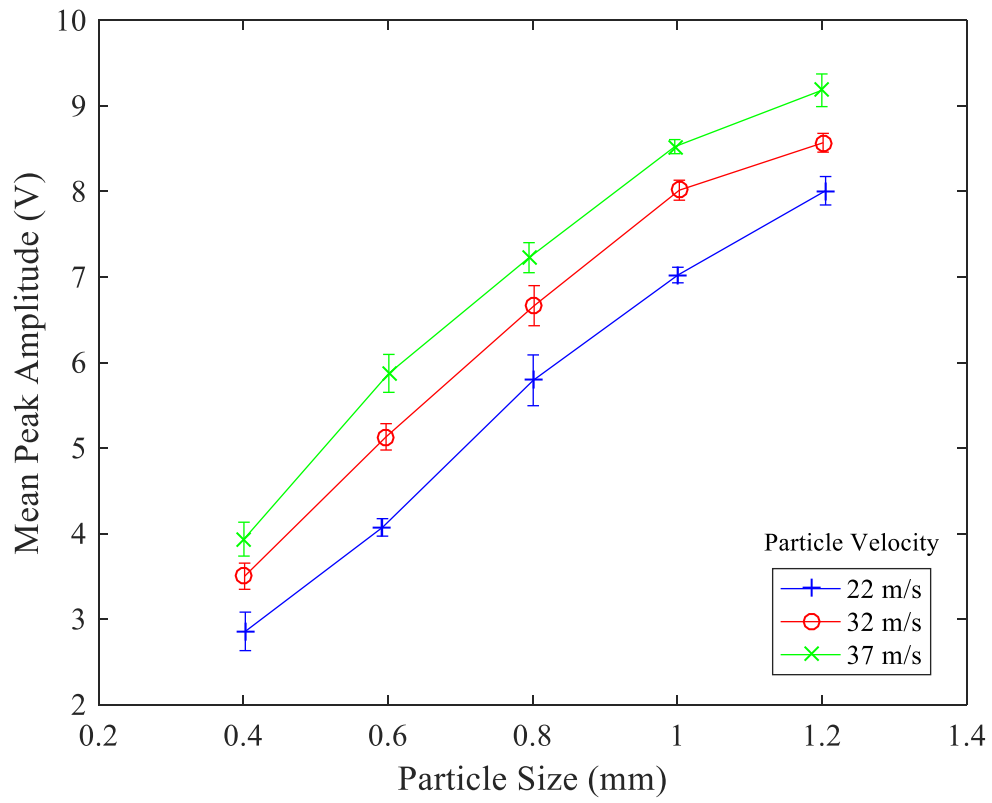


Fig. 9. Mean peak amplitude of the AE signals for different velocities.

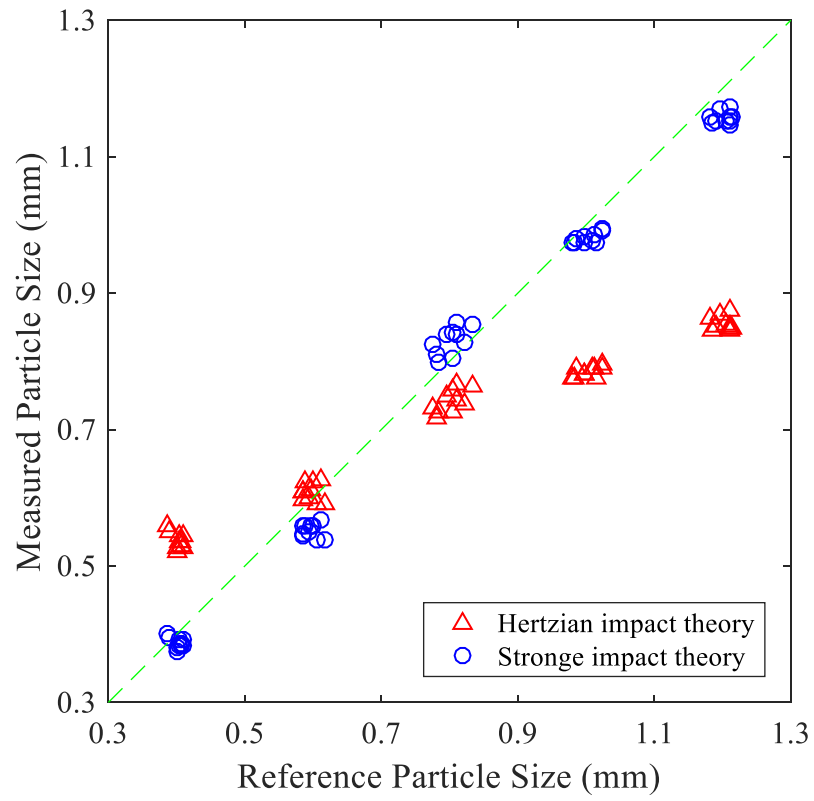


Fig. 10. Particle size inversion results using the two impact models (glass bead, $v=32$ m/s).

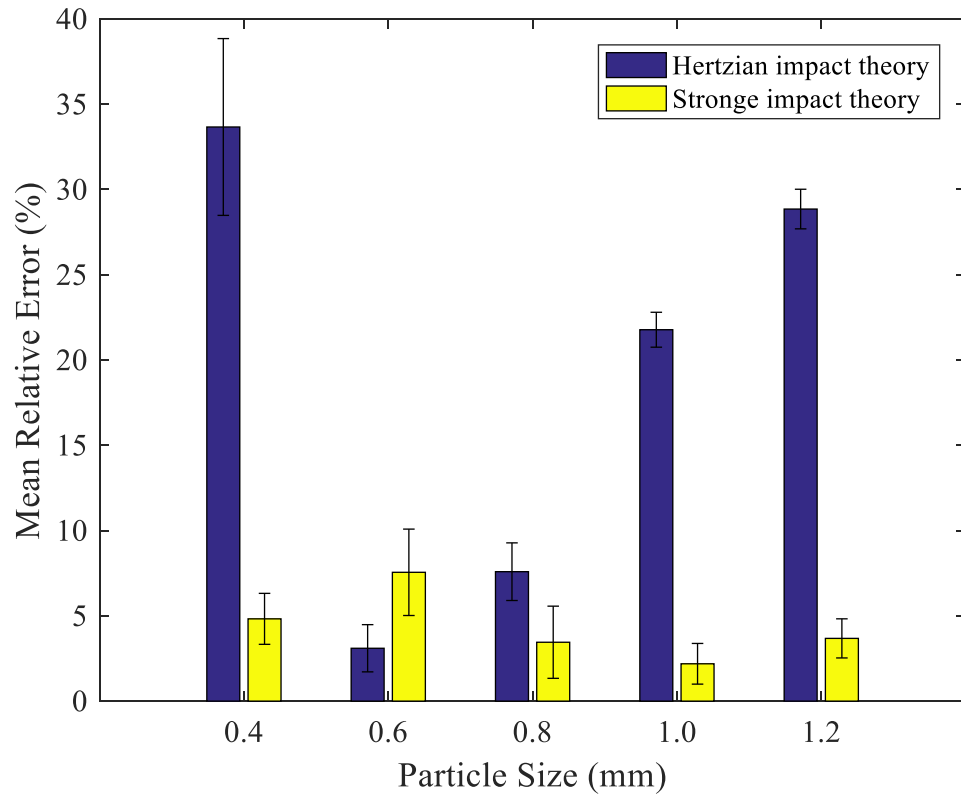


Fig. 11. Mean relative error of particle size inversion results.

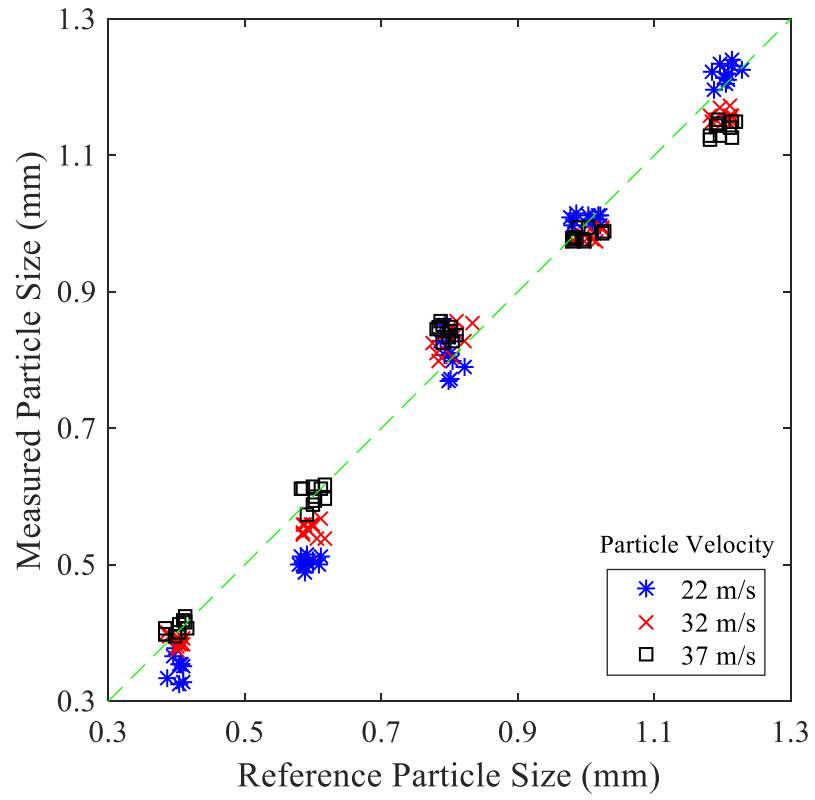


Fig. 12. Particle size inversion results.

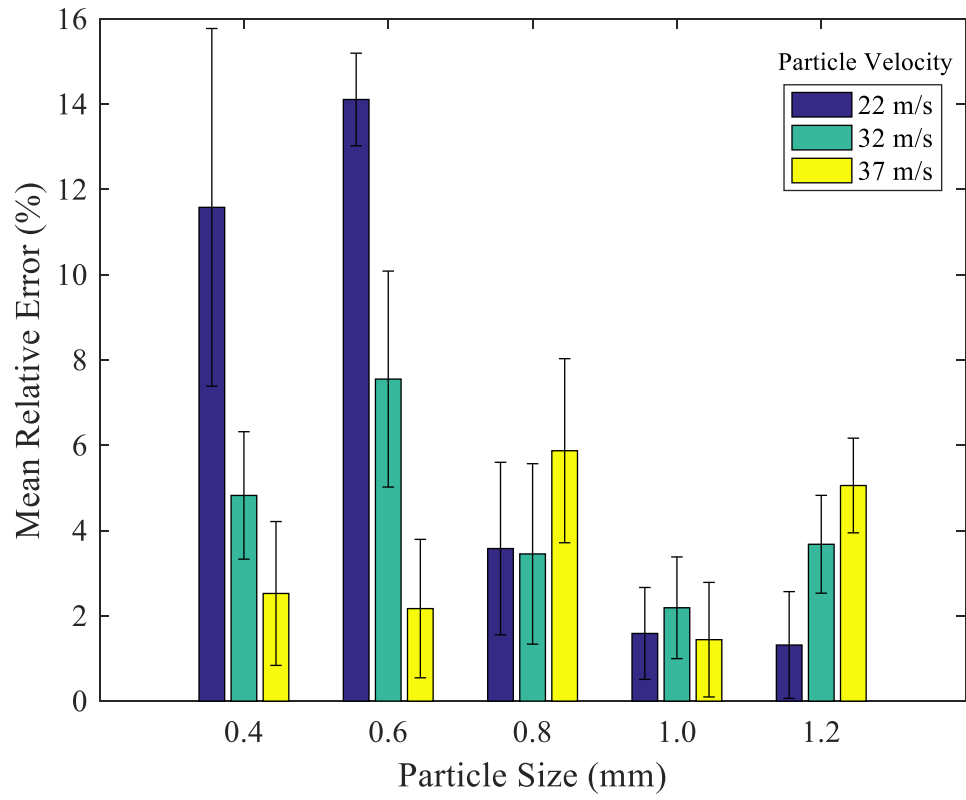


Fig. 13. Mean relative error with standard deviation for different particle sizes.

List of Tables:

Table I. Experimental conditions.

TABLE I
EXPERIMENTAL CONDITIONS

Particles	Mean diameter (mm)	Normalised standard deviation	Average velocity (m/s)	Normalised standard deviation
Set 1	0.4	2.4%	22.34	2.0%
			32.12	1.1%
			37.26	1.6%
Set 2	0.6	2.0%	22.17	2.9%
			31.66	2.1%
			37.11	1.9%
Set 3	0.8	1.6%	22.36	1.5%
			32.07	1.7%
			37.11	1.6%
Set 4	1.0	1.7%	22.26	2.2%
			31.90	1.3%
			37.18	1.5%
Set 5	1.2	1.1%	21.93	1.6%
			32.06	2.0%
			37.11	1.4%